Development of ECE Imaging System on LHD

Yuichiro KOGI, Takuya SAKODA, Atsushi MASE, Naoki ITO, Soichiro YAMAGUCHI[1)], Yoshio NAGAYAMA[1)] and Kazuo KAWAHATA[1)]

Art, Science and Technology Center for Cooperative Research, Kyushu University, Kasuga, Fukuoka 816-8580, Japan
[1)]*National Institute for Fusion Science, Toki, Gifu 509-5292, Japan*

(Received 4 December 2006 / Accepted 2 July 2007)

Electron cyclotron emission (ECE) imaging has been an important tool to investigate behaviors of temperature perturbations in the specific spatial area. So far, we have applied ECE detection system to a LHD plasma to measure electron temperature fluctuations in core region, however, it was difficult to distinguish perturbed temperature signals to a noise, which is naturally consisted in radiometry features and so on. Recently, we have optimized an ECE detector array especially in sensitivity to increase signal to noise ratio. An intermediate frequency(IF) system composed of commercial components have been replaced by an integrated system utilizing millimeter(microwave) integrated circuit technology(MIC) to fabricate a compact system maintaining the performance of the commercial system. As a result of application to the LHD plasma, we have successfully obtained ECE signal even in comparably low temperature operation sequence.

Keywords: electron cyclotron emission, imaging system, electron temperature measurement, millimeter wave, microwave, microwave integrated circuit technology

DOI: 10.1585/pfr.2.S1032

1. Inroduction

One of the unresolved issue in the plasma confinement is a clarification of various instabilities. Various methods utilizing electromagnetic wave with wavelength range around millimeter-wave have been developed to measure such instabilities. Measurement of electron cyclotron emission (ECE) is one of the main diagnostics to measure electron temperature. Temperature and density of fusion plasmas are high enough to consider the plasma as optically thick. The characteristic of the electron cyclotron emission is similar to the blackbody radiation when the plasma is optically thick where the ECE intensity is proportional to the local electron temperature. Therefore, the electron temperature and its fluctuations can be diagnosed by measuring the intensity of ECE. ECE imaging (ECEI) [1–5] is a promising method to measure 2 or 3 dimensional electron-temperature profile and its fluctuations precisely. We also have been dedicated to develop ECEI system [6] for visualization of the dynamic motion of electron temperature profile. In order to obtain well-resolved image, a high sensitivity (low noise) detector and a lot of detection channels like charge coupled device (CCD) in the digital camera are essential. In the previous system, we employed commercial components, such as antennas, microwave amplifiers, frequency-mixers and etc., to construct the imaging system. However, the spatial resolution becomes worse due to poor integration of ECE detecting antennas utilizing a pyramidal horn. Furthermore, ECEI system needs enormous number of high-cost functional millimeter wave (microwave) components to construct fine image. We have employed cost-effective millimeter (microwave) integrated circuit (MIC) technology to construct optimized system. In this article, we report the detail of constructed system by MIC technology and preliminary measurement results.

2. Schematics of the ECEI System

Schematic view of the ECEI system is shown in Fig. 1. The ECEI system is composed of quasi-optics, a detector array, and an intermediate frequency (IF) system. The ECE emitted from the plasma is introduced to the diagnostic port via an ellipsoidal mirror and a plane mirror installed inside the vacuum vessel. The direction of the ellipsoidal mirror can be adjusted in the poloidal plane by a rotator knob. The ECE with frequency over 70 GHz can propagate through two dichroic plates, and is focused onto the detector array. Since the magnetic field strength profile is a function of the radial position, frequency of the ECE is

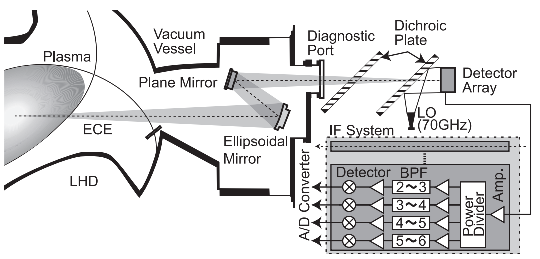

Fig. 1 Schematic view of the ECEI system.

author's e-mail: kogi@astec.kyushu-u.ac.jp

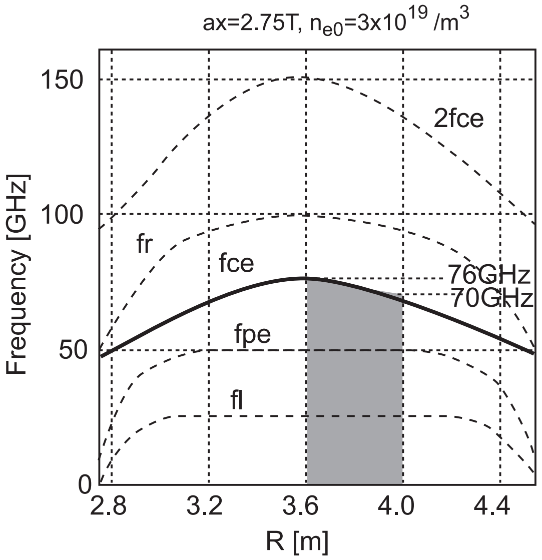

Fig. 2 Characteristic frequency of the LHD.

also a function of radial position as shown in Fig. 2. The frequency range from 70 to 76 GHz corresponds to radial position from 3.6 to 4.0 m when the fundamental frequency of the ECE is detected. The dichroic plate located just outside of the diagnostic port is utilized to distinguish the ECE with frequency over 70 GHz from the reflected wave with frequency below 69 GHz, which is utilized by the microwave imaging reflectometer (MIR). Another dichroic plate is utilized to combine the ECE with a local oscillator (LO) wave (70 GHz). In the receiver array, matrix array of a detector is arranged to resolve emission points in the troidal and poloidal plane. The LO wave and the ECE are mixed in the detector, and then IF signals are generated. This process will be described in Sec. 3. The IF signals are further fed to the IF system, which is consisted from band-pass filter bank to resolve the ECE frequency in radial direction. Each output of the filtered signals corresponds to the frequency of the ECE, i.e., radial emission point. The IF system also provides low noise amplifiers and video detectors for transformation of the IF signal to further low frequency (DC-MHz) level.

3. Integration of the ECEI System

Figure3 shows the detector element consisted of four patch antennas, eight parasitic elements [7], one mixer diode, and one ECE rejection filter. This detector element is fabricated on the Teflon substrate with t = 127 um and $\varepsilon_r = 2.2$. These planar circuit components are designed by using microwave EM simulator (MW Office and Sonnet). The 10 % broadening of the bandwidth of each antenna is achieved by careful gap adjustment between the patch antennas and the parasitic elements and size of the parasitic patch. Symmetric arrangement of four patch antennas contributes to symmetric Gaussian detection pattern of the antenna. The ECE (70-76 GHz) and the LO (70 GHz)

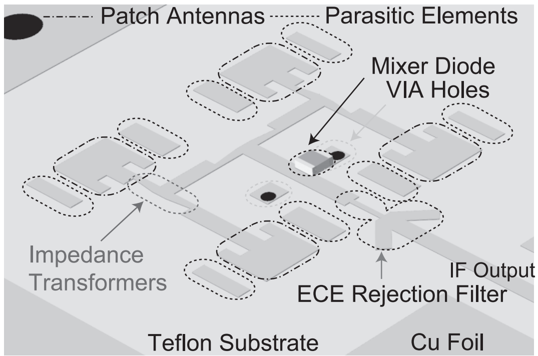

Fig. 3 Layout of the detector element.

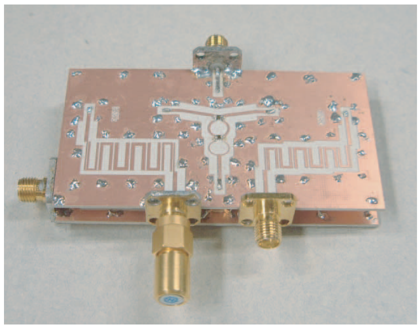

Fig. 4 Picture of part of the integrated IF system.

wave detected by the each antenna are combined by the impedance transformers, and are mixed by the Schottoky barrier diode with cutoff frequency of 2 THz. DC current of several hundred microamperes biases the diode. The ECE and the LO wave are confined inside the mixer and the antenna region by the ECE rejection filter. Location of the diode and the filter is also adjusted in order to optimize the IF signal and to match the impedance of the antennas to 50 ohm. Only the IF signal with frequency up to 10 GHz can pass through the filter and reach the IF output port. In the present experiment, three sets of the detector element, which are linearly arranged, are integrated on the substrate.

Figure 4 shows a picture of the part of the IF system for 1 detector element. In the present stage, we could integrate the system except for the video detector. 4-way broadband Wilkinson power divider (located at the center of top and bottom substrate) and quarter-wavelength microstrip line coupling filter [8] (located at both side of top and bottom substrate) are employed, and are designed by the simulator. The center frequencies of these filters are 2.5, 3.5, 4.5, and 5.5 GHz with a bandwidth of 0.8 GHz, respectively. It is not indicated in Fig. 4, hetero-junction bipolar (HBT) amplifier with bandwidth from 1 to 6 GHz and power gain over 15 dB is also integrated on another substrate to adjust the signal level. Total gain of the amplifier is 60 dB by using two or three stage HBT amplifiers and a help of commercial broadband amplifier. Example of the system characteristic is shown in Fig. 5. This pre-experiment is performed by composing of the integrated

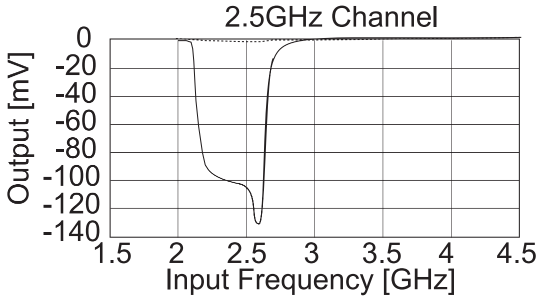

Fig. 5 Detector output characteristics from 2.5 GHz band pass frequency by the pre-experiment.

ECE detector and the IF system. Instead of the ECE, a millimeter-wave source with fixed frequency from 72 to 76 GHz and power of 0 dBm is injected into the detector by a pyramidal horn. Distance between the horn and the detector is 0.2 m. It is noted that total gain of this IF system decreases drastically to 30 dB. A solid line indicates the characteristics of the IF output. While, a broken line indicates the system noise level, when the source is not injected. It is found that the signal level within the bandwidth of the band-pass filter increases. It is also confirmed that the signal level can be distinguished from noise level of the system.

4. Application to LHD Plasma

We have applied our integrated system to LHD plasma as shown in Fig. 1. Figure 6 shows the results of initial measurement. Time sequences of the heating systems (a, b), line-integrated density by FIR(c), electron temperature by Tomson scattering (d), detector output by the present integrated system (e), and detector output by the same type ECE detector and the previous IF system composed of coaxial components (f) are indicated from top to bottom. Maxima of electron density and temperature in the core region attained $2.2 \times 10^{19}\,m^{-3}$ and 3.75 keV, respectively. It is confirmed that the increment of the signals when the plasma is present, which is considered to be proportional to electron temperature.

In order to confirm the performance of the developed IF system, an IF system composed of commercial microwave components is also applied at the same time as described before. Frequencies specified on the figure indicate center frequencies of the band-pass filters. Level of the detector output without plasma is considered as noise level, since the source of noise is dominated by amplifiers and video detectors without plasma emission. Signal to noise ratio in the case of commercial components seems to be comparable to that in the case of newly developed MIC-IF system. From these results, we have confirmed that developed IF system has a similar performance to that of the IF system with commercial components. Minimum measurable temperature level of this system is estimated as follows. The decrement of the detector output of 3.5 GHz

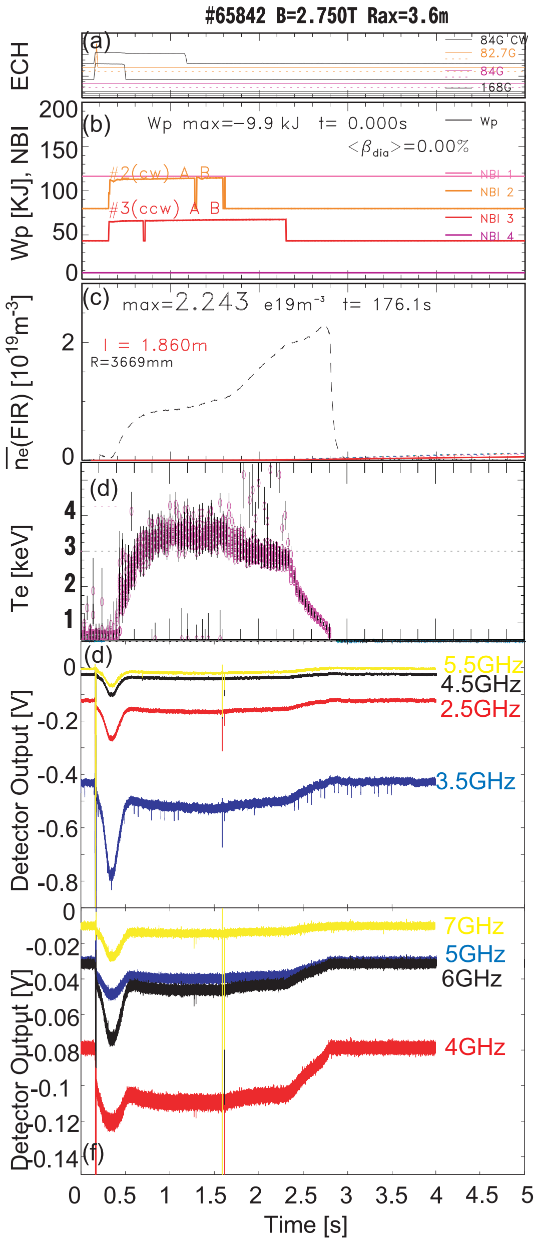

Fig. 6 Time sequences of the heating systems (a, b), line density by FIR(c), electron temperature by Tomson scattering(d), detector output by the integrated system (e), and detector output by the commercial system (f) are indicated from top to bottom.

channel from the noise floor(−0.43 V) is 0.1 V at 1.5 s, which is considered to correspond to electron temperature of 3.5 keV measured by Tomson scattering. While the effective voltage of the envelope of the detector output is about 0.007 V, which is considered to be a minimum measurable temperature when electron temperature fluctuation is not detected. The detector output of 0.007 V corresponds to 250 eV. This minimum measurable temperature relates to integration time of the video detector or low-pass filter attached just after the video detector. Precise evaluation of signal to noise ratio performance will be performed by using a hot–load noise source in the future. We consider this minimum measurable temperature is still too high to visualize phenomena of the electron temperature fluctuations. This undesired condition will be improved by installing a mechanical shutter in front of the diagnostic port to prevent the surface of the window from being coated by sputtering due to impurities.

The reduction of 30 dB in transmission loss is estimated by removing the coated impurities, which implies that the improvement of the S/N ratio of thousand times is also expected.

5. Summary and Future Work

In summary, almost all components of the system have been integrated by MIC technology to compose the ECEI system with better resolution. The system with high sensitivity, compact, and low cost has been achieved. We have applied our integrated ECE measurement system to LHD plasmas, and confirmed that the signal, which is proportional to electron temperature, is observed.

In the future, we plan to extend the system, i.e., increment of detector channels (5 by 5), with more compact and lower loss IF system.

Acknowledgements

This work is performed as a collaborating research program at National Institute for Fusion Science (NIFS03KCHP003), and is also partly supported by the Grant-in-Aid for Scientific Research, the Ministry of Education, Science, Sports and Culture ("Advanced Diagnostics for Burning Plasma" No. 16082205)

[1] R.P. Hsia *et al.*, Rev. Sci. Instrum. **68**, 488(1997).
[2] B.H. Deng *et al.*, Rev. Sci. Instrum. **70**, 998 (1999).
[3] B.H. Deng *et al.*, Rev. Sci. Instrum. **72**, 301 (2001).
[4] H. Park *et al.*, Rev. Sci. Instrum. **75**, 3787 (2004).
[5] C.W. Domier *et al.*, Rev. Sci. Instrum. **77**, 10E924 (2006).
[6] A. Mase *et al.*, Rev. Sci. Instrum. **74**, 1445 (2003).
[7] S. Haider *et al.*, *Microstrip Patch Antennas for Broadband Indoor Wireless Systems* (Depart of Electrical & Electronics Engineering, Part4 Project Report) 2003.
[8] G. Matthaei *et al.*, *MICROWAVE FILTERS, IMPEDANCE-MATCHING NETWORKS, AND COUPLING STRUCTURES* (Artech House) p.422.